Onset of microbial influenced corrosion (MIC) in stainless steel exposed to mixed species biofilms from equatorial seawater

Prasanna Jogdeo[1,2], Rosalie Chai[1], Sun Shuyang[3], Martin Saballus[4], Florentin Constancias[1], Sudesh L Wijesinghe[5,6], Dominique Thierry[7], Daniel J Blackwood[5], Diane McDougald[1,3], Scott A Rice[1,3,8] and Enrico Marsili[1,9*],

[1]*Singapore Centre for Environmental Life Sciences Engineering, NTU, Singapore*

[2]*Interdisciplinary Graduate School, Nanyang Technological University, Singapore*

[3]*ithree Institute, University of Technology Sydney, Australia*

[4]*Technical University of Dresden, Dresden, Germany*

[5]*Department of Materials Science & Engineering, NUS, Singapore*

[6]*Singapore Institute of Manufacturing Technology (SIMTech)*

[7]*French Corrosion Institute, Brest, France*

[8]*School of Biological Sciences, NTU, Singapore*

[9]*School of Chemical and Biomedical Engineering, NTU, Singapore*

Keywords – Microbially influenced corrosion (MIC), Biofilms, Stainless steel, Mixed microbial community, Seawater

Abstract

The understanding of microbial influenced corrosion (MIC) in aerobic mixed biofilms benefits from advanced microscopy and microbial ecology characterization of biofilms. Here, the onset of MIC in stainless steel coupons was studied in both natural and artificial seawater. Rapid selection of biofilm-forming microorganisms from natural seawater was observed for field experiments. Potential ennoblement was observed only in natural seawater. A seawater derived mixed microbial consortium enriched in artificial seawater was used to characterize the effect of several parameters on MIC. The concentration of organic carbon was the major determinant of MIC, while shaking speed and polishing played minor roles. The biofilm was preferentially formed at the grain boundaries. These results outline the need for MIC onset characterization with mixed microbial consortia to predict long-term corrosion behaviour of stainless steel in seawater.

Introduction

Microbially influenced corrosion (MIC) of metals refers to the involvement of microorganisms in the metal deterioration process. MIC has significant economic consequences for industries such as oil and gas, mining, logistics and waste water treatment, with social and environmental impacts associated with the deterioration of materials[1].

Microorganisms affect physicochemical reactions at the metal/liquid interface, either slowing down or accelerating abiotic corrosion processes[1, 2]. Due to their physicochemical[3] and microbiological resistance[4] to metal deterioration and MIC, stainless steels (SS) are used in key marine components.

MIC mechanisms previously put forth include the effects of differential concentrations of oxygen and nutrients; generation of corrosive metabolites or by-products; alteration of anion ratios and inactivation of corrosion inhibitors[5]. Adsorbed extracellular biofilm matrix molecules such as proteins, lipids, humic acids and polysaccharides change the SS surface by modifying surface charge, wettability or surface energy, thus enhancing or inhibiting MIC[6]. The biofilm can also act as a diffusional barrier preventing oxygen and corrosive substances from reaching the metal surface[7].

Sulphate-reducing bacteria (SRB) are commonly cited as the primary organisms responsible for MIC under anaerobic and anoxic conditions in seawater through the production of corrosive sulphides. However, aerobic microorganisms have also been increasingly studied, substantiating their role in MIC process. For example, in the presence of the aerobic marine bacterium *Pseudomonas* sp., SS304 showed a higher corrosion rate and lower resistance of the passive film, indicating localised breakdown of passive film, in contrast with abiotic experiments with stable and passivating Cr-enriched oxide films [8]. Microbial activities can alter the inorganic passive layer and increase metal dissolution. Extensive micro-pitting corrosion was observed underneath biofilms. A negative shift in the corrosion potential was observed along with an increase in current density for duplex 2205 steel in presence of marine, halophilic *Pseudoalteromonas* sp.[9].

Most studies on MIC have focused on axenic cultures, rather than the mixed microbial communities commonly occurring in the environment. In pure culture studies, both corrosion-enhancing and corrosion-protecting effects have been reported in artificial seawater [2, 5, 10, 11]. *Vibrio neocaledonicus*, an aerobic marine bacterium has been reported to reduce corrosion of carbon steel ASTM A36 by sixty-fold[12]. Corrosion inhibition by this bacterium was first reported by Pederson et. al in 1988[13]. The corrosion inhibition effect of *Pseudomonas fragi* of AISI 1018 steel has been linked with oxygen depletion due to the formation of a uniform biofilm[14]. *Bacillus* sp. and *Hafnia alvei* have been shown to reduce mild steel corrosion after prolonged exposure[15], and *Pseudomonas* S9 and *Serratia*

marcescens EF190 were reported to decrease corrosion of ASTM A619 carbon steel under aerobic conditions [16].

In contrast to typical laboratory conditions using axenic cultures, marine microorganisms at liquid/solid interfaces exist as structurally and functionally organized communities[17]. These communities often occur as biofilms, and are spatially and chemically heterogeneous[18]. The effect of a mixed microbial biofilm on MIC differs from that of single species biofilms[19]. For example, exposure to a triculture of an acetogenic bacterium, *Eubacterium limosum*, and 2 *Desulfobacter* sp. strains showed the greatest increase in corrosion rate of carbon steel, followed by a co-culture of *E. limosum* and *Desulfovibrio* sp., while a single species culture of *E. limosum* increased corrosion rates the least [20]. Hence, although studying single species may help to understand specific steps of MIC mechanisms, mixed microbial biofilms are more representative of the natural environment.

There are only few studies focusing on MIC in aerobic marine biofilms in natural seawater. Early studies showed that discontinuous biofilm on AISI 316 SS alters local corrosion potential and initiates pit corrosion[21]. It was hypothesized that MIC of SS was due to the oxygen reduction depolarization[22]. The complexity of MIC mechanisms in the presence of seawater biofilms was addressed with the combination of electrochemistry and surface analysis [23]. However, a deep understanding of microbial ecology and physiology is needed to deconvolute the individual MIC mechanisms in biofilms[24].

For a laboratory system, in addition to the microbiological aspects, several other parameters also impact the corrosion process, including using a batch or continuous system, flow conditions in a continuous system, type of metal used, metal surface pre-treatment and oxic or anoxic conditions[25]. Using a continuous flow cell system, Duncan et al. studied the effects of corrosion inhibitors on MIC of mild steel[26]. A recent co-culture study with *V. natriegens* and *Shewanella oneidensis* was conducted in a flow system using a microfluidic device [27]. Surface topography influences the abiotic corrosion reactions [28, 29] as well as adhesion of the biofilm[30], which in turn affects corrosion rate. Bacterial settlement is influenced by substratum roughness and geometry [31]. Bacteria settled preferentially on the depressions of the oxide film grain boundaries of 316 SS [32].

As MIC is a complex process involving material science, chemistry and microbiology, it is necessary to implement a multidisciplinary approach [25]. Here, we studied the MIC onset of UNSS2507 in natural seawater Following these experiments, a defined marine microbial community enriched from sea water was used in a laboratory batch system to assess onset of corrosion on SS304 coupons. The results show potential ennoblement in natural seawater. Furthermore, the carbon source concentration is the primary determinant of the MIC and the biofilm accumulated at the SS grain boundaries.

Materials and Methods

Sample preparation

The austenitic grade 304 (UNS S30400: Cr 18%, Ni 8%) used for laboratory experiments and the duplex grade 2507 (UNS S32750: Cr 24-26%, Ni 6-8%, Mo 3-5%, Cu 0.5%) used for environmental experiments as received, were purchased from A-plus Engineering, Singapore (Table 1). To assess the effects of surface roughness, SS304 coupons were polished with sandpaper, grit size p600 or p1000 (ISO/FEPA Grit designation), subsequently soaked in 80% acetone for 15 min and sonicated for 7 min in 100% ethanol. All other coupons were polished with p600 grit sandpaper and cleaned as mentioned previously.

Enriched mixed marine microbial community

The enriched microbial community for laboratory experiments was obtained by inoculating 10 mL of coastal seawater into minimal marine medium (3M), composed of 920 mL 0.5X nine salt solution (17.6 g NaC1; 1.47 g Na_2SO_4; 0.08 g $NaHCO_3$; 0.25 g KCl; 0.04 g KBr; 1.87 g $MgC1_2{\cdot}6H_20$; 0.41 g $CaC1_2{\cdot}2H_20$; 0.01 g $SrCI_2{\cdot}6H_20$; 0.01 g H_3BO_3), 10 mL (0.4 M Tricine + 1 mM $FeSO_4$), 10 mL of 952 mM NH_4Cl, 10 mL of 132 mM K_2HPO_4, 10 mL of 20% glucose, buffered with 40 mL of 40 mM MOPS (3-morpholinopropane-1-sulfonic acid). After one week of sub-culturing, frozen stocks of the mixed microbial community were prepared and used for laboratory experiments.

Corrosion cells

The corrosion cells were fitted with three SS coupons (1 x 1 x 0.2 cm) as working electrodes, a Ti coil common counter electrode and a Ag/AgCl (saturated KCl) common reference electrode. In the following, all electrochemical potentials are reported with respect to Ag/AgCl (saturated KCl). One mL of enriched mixed microbial community was inoculated into the 120 mL corrosion cells. The corrosion cells were incubated on a rotary shaker at 0 to

80 rpm, at room temperature (~22°C) for 7 or 35 days. Every 2nd and 4th day for the 7 day experiments and every 5 days for the 35 day experiments, 50% of the spent growth medium was replaced with fresh growth medium to reduce the concentration of suspended cells, provide fresh nutrients and maintain circum-neutral pH.

Electrochemical analysis, biofilm visualisation and surface analysis

Linear Sweep Voltammetry (LSV) at a scan rate of 0.166 mV/s from -800 to -100 mV was performed using a multichannel potentiostat (VSP biologic, France), and corrosion current density (j_{corr}) and corrosion potential (E_{corr}) were calculated using the Tafel equation.

The biofilms on the coupon surfaces were stained with the LIVE/DEAD® BacLight™ Bacterial Viability Kit and imaged by CLSM at 400 × magnification (LSM780, Zeiss). The reflection technique was used here to visualize the metal surface[33]. The coupons were also imaged by Field Emission Scanning Electron Microscopy (FESEM, JEOL 7600F, USA) after 35 days. Atomic force microscopy (AFM) was performed to assess surface roughness of polished coupons using Bioscope Catalyst AFM (Bruker), in tapping mode.

DNA extraction

Coupons immersed in coastal seawater (St. John's Island, Singapore), were retrieved after 1 h, 2 days and 7 days. DNA was extracted from biomass retrieved from the surface using the FastDNA® SPIN Kit for soil. 27F and 1492R primers were used for a PCR and the products were sent for amplicon sequencing.

Results and Discussion

The unpolished UNSS32750 coupons were immersed in tanks circulated with sand filtered seawater (~29°C) at flow rate of 300 $Lday^{-1}$. The E_{corr} increased and then stabilized after 2 days at 268 ± 8 mV (Figure 1d), indicating potential ennoblement. Increases in potential are consistent with previous experiments in flowing seawater under equatorial conditions, where the E_{corr} increased to 350 mV vs. Ag/AgCl [34]. CLSM images after 1 h show individual cells on the coupon surface, multiple layers of bacteria after 2 days and aggregated colonies after 7 days (Figure 1 a, b, c). Surface coverage of the biofilm increased from 16.3 ± 4.4% after 1 h to 25.8 ± 13.4 % after 7 days. The variability of biofilm coverage after 7 days reflects the variety of factors that affect biofilm structure, especially in mixed microbial consortia [35]. The microbial community composition of the biofilm (n = 2) formed on the metal surface after 1 h of deployment was different from that of the sea water community, with an enrichment in

172 *Gammaproteobacteria* (SJ3), without further changes until 7 days. A 64% reduction in
173 unknown *Proteobacteria* (SJ1), which was abundant in seawater, was seen in the biofilm
174 formed after 1 h with a slight increase at 7 days. Approximately a 90% decrease was seen in
175 unknown *Bacteria* (SJ2) after 1 h of deployment (Figure 2).
176
177 Due to the corrosion resistance of UNSS32750 [36], the less-resistant UNSS30400 was selected
178 for further experiments in 3M with 0.2% glucose as carbon source. The E_{corr} after inoculation
179 reached -700 ± 10 mV within 10 days and then remained stable over 35 days. In abiotic
180 controls, E_{corr} decreased to -400 ± 3 mV after 15 days and remained constant for 35 days
181 (Figure 3b). While the E_{corr} alone cannot be used to predict the corrosion likelihood of
182 UNSS30400[17] , it is interesting to note that the E_{corr} observed in our experiment was similar
183 to that recorded in anaerobic corrosion tests involving SRB [37, 38]. The j_{corr} increased to 2.3 µA
184 cm^{-2} at 10 days and then remained constant over 35 days (n = 3). The sterile controls showed
185 very low j_{corr} (~0.2 µA) throughout the experiments (Figure 3 a). The low corrosion current is
186 comparable with previous studies on aerobic corrosion and is consistent with the lack of
187 anaerobic microorganisms in the starter community, particularly SRBs. The microstructural
188 variability of biofilms with time [18] likely results in large j_{corr} variation across independent
189 biological replicates.
190
191 After 35 days, the biofilm and coupon surface were visualised using CLSM and SEM. CLSM
192 images showed that 15 µm thick biofilms accumulate at the grain boundaries (Figure 4). This
193 observation was confirmed by the analysis of intensity profiles of stainless steel and biomass,
194 compared to determine their respective localization (Figure 5) A previous CLSM study
195 reported low coverage of mushroom-like biofilms on ennobled SS coupons and uniform, thin
196 biofilms on non-ennobled samples [39]. Bacteria preferentially colonized the grain boundaries
197 on stainless steel [40], suggesting that intergranular MIC might contribute to the overall
198 corrosion. However, intergranular corrosion (IGC) also has chemical causes, thus further
199 investigation is required to determine the actual role of biofilms in IGC [41]. FESEM images of
200 control coupons revealed small grain structure with shallow boundaries as compared to
201 coupons imaged on 35 days following biofilm removal (Figure 6). This observation was
202 consistent with pit deepening in steel samples exposed to marine biofilms [42, 43]. Previous
203 AFM analysis [32] showed that grain boundaries on 316L harbour bacteria and that bacterial
204 colonization depleted Cr and Fe, promoting localised attack on the alloy. EDX results (data
205 not shown) showed lower carbon content and higher Fe and Cr associated with control

UNS30400 coupons compared to those with biofilms, while oxygen and sulphur were detected only on samples exposed to biofilms, indicating the formation of a thicker oxide layer and biomass accumulation, respectively. Furthermore, carbon-rich biomass localizes preferentially at the grain boundary, thus confirming the CLSM results.

As both j_{corr} and E_{corr} stabilized within 10 days, further experiments were performed over 7 days to focus on the onset of corrosion. A typical set of Tafel plots with time is shown in (Figure 7). To determine the effect of nutrient concentration, sterile filtered seawater (~0.002% glucose [44]) was compared with 3M medium (0.2 % glucose). The j_{corr} for 3M medium was much higher than in seawater (Figure 8a). The effect of inorganic vs. organic medium was previously studied in single culture experiments [45] and it was concluded that inorganic medium favours biofilm production, thus protecting metal from corrosion, while organic medium promotes corrosion. Although our results are taken in very different experimental conditions (mixed biofilm), it is possible that abundance of organic nutrient shifts biomass from the biofilm to the planktonic phase, thus increasing corrosion[46].

The surface roughness (Ra) of unpolished or polished (P600 or P1000) UNS S30400 coupons were of 185 ± 20, 173 ± 50 and 93.2 ± 5 nm, respectively. Following polishing, the coupons were soaked in sterile 3M for 4 days to obtain a stable passivation layer, and then inoculated as described. The surface preparation neither affected E_{corr} nor j_{corr} (Figure 8 e,f).

Diffusional limitations affect the biofilm life cycle [47] and community composition [48]. As oxygen is rapidly depleted in both the biofilm and planktonic phases, due to bacterial growth, it is likely that the passive film on the stainless steel weakens, thus making the surface more vulnerable to corrosion [49]. Shaking increases aeration and nutrient delivery to the biofilm [50] and facilitates removal of reaction products from the metal surface, thus enhancing corrosion current. Without shaking, j_{corr} was 47% and 52% lower after 7 days than at 40 rpm and 80 rpm shaking, respectively (Figure 8c). Similarly, E_{corr} without shaking was higher by 200 mV than with shaking, indicating that diffusional limitations determine MIC onset (Figure 8d). Shaking affects biofilm structure, resulting in thinner and more resilient biofilm. It has been shown that uniform biofilms obstruct oxygen diffusion, enhancing corrosion inhibition[51]. Microsensors experiments, which measure oxygen concentration within biofilms, are needed to deconvolute the effect of diffusional limitations from biofilm structure in enhancing/reducing the corrosion current.

Conclusions

In equatorial seawater, biofilm-forming microorganisms were rapidly selected on SS coupons from the planktonic community. Surface ennoblement was observed only in seawater. In the laboratory, the MIC onset of SS coupons exposed to mixed microbial biofilms enriched from seawater was characterised for surface finish and nutrient composition in both 3M and sterile seawater. The corrosion current density increased in glucose-rich 3M, as the rapid bacterial growth scavenges oxygen, likely weakening the oxide layer on the SS surface. CLSM, SEM imaging and EDX analysis show the accumulation of a biofilm at the grain boundaries. Metatranscriptomics experiments are ongoing to determine which microorganisms in the biofilms actively contribute to the MIC process.

Acknowledgements

Research supported by the Singapore National Research Foundation and Ministry of Education under the Research Centre of Excellence Programme. PJ was supported by IGS-NTU. RC is funded through a 'Singapore Ministry of Education, Academic Research Fund Tier 1 RG141/15'. Additional support was provided by the National Research Foundation of Singapore (MSRDP-12). We thank Dr. Hongjie An for his help with AFM measurements.

References

1. B. Little, J. Lee, and R. Ray, *Biofouling,* **23** (1-2), 87-97 (2007).
2. N. Kip and J. A. van Veen, *ISME J,* **9** (3), 542-551 (2015).
3. R. E. Melchers and R. Jeffrey, *Corrosion,* **60** (1), 84-94 (2004).
4. H. H. P. Fang, L.-C. Xu, and K.-Y. Chan, *Water Research,* **36** (19), 4709-4716 (2002).
5. R. Zuo, *Appl Microbiol Biotechnol,* **76** (6), 1245-1253 (2007).
6. S. Chongdar, G. Gunasekaran, and P. Kumar, *Electrochimica Acta,* **50** (24), 4655-4665 (2005).
7. D. M. Vaughn-Thomas, (1988).
8. S. Yuan, S. Pehkonen, Y. Ting, E. Kang, and K. Neoh, *Industrial & Engineering Chemistry Research,* **47** (9), 3008-3020 (2008).
9. M. Moradi, Z. Song, L. Yang, J. Jiang, and J. He, *Corrosion Science,* **84** 103-112 (2014).
10. K. Alasvand Zarasvand and V. R. Rai, *International Biodeterioration & Biodegradation,* **87** 66-74 (2014).
11. S. Dobretsov, R. M. Abed, and M. Teplitski, *Biofouling,* **29** (4), 423-441 (2013).
12. M. Moradi, Z. Song, and X. Tao, *Electrochemistry Communications,* **51** 64-68 (2015).

13. A. Pedersen, S. Kjelleberg, and M. Hermansson, *Journal of microbiological methods,* **8** (4), 191-198 (1988).
14. A. Jayaraman, E. Cheng, J. Earthman, and T. Wood, *Applied microbiology and biotechnology,* **48** (1), 11-17 (1997).
15. R. Jack, D. Ringelberg, and D. White, *Corrosion science,* **33** (12), 1843-1853 (1992).
16. A. Pedersen and M. Hermansson, *FEMS Microbiology Letters,* **86** (2), 139-148 (1991).
17. B. J. Little, J. S. Lee, and R. I. Ray, *Electrochimica Acta,* **54** (1), 2-7 (2008).
18. J. Wimpenny, W. Manz, and U. Szewzyk, *FEMS Microbiology Reviews,* **24** (5), 661-671 (2000).
19. S. M. Beech I. B. , Gaylarde C. C. , Smith W. L. , Sunner J., in *Understanding Biocorrosion: Fundamentals and Applications*, p. 33-50, (2014).
20. S. A. B. N. J. E. Dowling, T. J. Phelps and D.C. White, *Journal of Industrial Microbiology,* **10** (1992), 207-215 (1992).
21. S. Dexter and G. Gao, *Corrosion,* **44** (10), 717-723 (1988).
22. A. Mollica, *International biodeterioration & biodegradation,* **29** (3-4), 213-229 (1992).
23. F. Mansfeld, G. Liu, H. Xiao, C. Tsai, and B. Little, *Corrosion science,* **36** (12), 2063-2095 (1994).
24. I. B. Beech and J. Sunner, *Current opinion in Biotechnology,* **15** (3), 181-186 (2004).
25. S. Wade, M. Javed, E. Palombo, S. McArthur, and P. Stoddart, *International Biodeterioration & Biodegradation,* **121** 97-106 (2017).
26. K. E. Duncan, B. M. Perez-Ibarra, G. Jenneman, J. B. Harris, R. Webb, and K. Sublette, *Applied microbiology and biotechnology,* **98** (2), 907-918 (2014).
27. S. P. Kotu, C. Erbay, N. Sobahi, A. Han, S. Mannan, and A. Jayaraman, *in* "CORROSION 2016". NACE International, 2016.
28. A. Y. Kandeil and M. Y. Mourad, *Surface and Coatings Technology,* **37** (2), 237-250 (1989).
29. T. Hong and M. Nagumo, *Corrosion Science,* **39** (9), 1665-1672 (1997).
30. E. Medilanski, K. Kaufmann, L. Y. Wick, O. Wanner, and H. Harms, *Biofouling,* **18** (3), 193-203 (2002).
31. P. E. Cook and C. C. Gaylarde, *International Biodeterioration,* **24** (4-5), 265-270 (1988).
32. G. Geesey, R. Gillis, R. Avci, D. Daly, M. Hamilton, P. Shope, and G. Harkin, *Corrosion Science,* **38** (1), 73-95 (1996).
33. T. R. Neu and J. R. Lawrence, *FEMS Microbiology Ecology,* **24** (1), 11-25 (1997).
34. M. Eashwar, G. Sreedhar, A. Lakshman Kumar, R. Hariharasuthan, and J. Kennedy, *Biofouling,* **31** (6), 511-525 (2015).
35. P. S. Stewart and M. J. Franklin, *Nature Reviews Microbiology,* **6** (3), 199-210 (2008).

36. D. Shifler, S. Fujimoto, H. Kihira, F. Martin, and D. Shifler, *The Electrochemical Society, Inc., Nueva Jersey, Estados Unidos,* 345-354 (2005).
37. X. Sheng, Y.-P. Ting, and S. O. Pehkonen, *Corrosion Science,* **49** (5), 2159-2176 (2007).
38. S. Yuan, B. Liang, Y. Zhao, and S. Pehkonen, *Corrosion Science,* **74** 353-366 (2013).
39. M. Mattila, L. Carpen, T. Hakkarainen, and M. S. Salkinoja-Salonen, *International Biodeterioration & Biodegradation,* **40** (1), 1-10 (1997).
40. K. R. Sreekumari, K. Nandakumar, and Y. Kikuchi, *Biofouling,* **17** (4), 303-316 (2001).
41. M. James and D. Hattingh, *Engineering Failure Analysis,* **47** 1-15 (2015).
42. H. Li, E. Zhou, D. Zhang, D. Xu, J. Xia, C. Yang, H. Feng, Z. Jiang, X. Li, and T. Gu, *Scientific reports,* **6** (2016).
43. D. Xu, J. Xia, E. Zhou, D. Zhang, H. Li, C. Yang, Q. Li, H. Lin, X. Li, and K. Yang, *Bioelectrochemistry,* **113** 1-8 (2017).
44. J. Lyman and R. H. Fleming, *J. mar. Res,* **3** (2), 134-146 (1940).
45. A. Rajasekar and Y.-P. Ting, *Industrial & Engineering Chemistry Research,* **50** (22), 12534-12541 (2011).
46. K. M. Thormann, R. M. Saville, S. Shukla, and A. M. Spormann, *Journal of bacteriology,* **187** (3), 1014-1021 (2005).
47. A. Kraigsley, P. Ronney, and S. Finkel, *Retrieved May,* **28** (2008).
48. J. R. Lawrence, M. R. Chenier, R. Roy, D. Beaumier, N. Fortin, G. D. W. Swerhone, T. R. Neu, and C. W. Greer, *Applied and Environmental Microbiology,* **70** (7), 4326-4339 (2004).
49. D. Chen, E.-H. Han, and X. Wu, *Corrosion Science,* **111** 518-530 (2016).
50. L. E. McDaniel and E. G. Bailey, *Applied Microbiology,* **17** (2), 286-290 (1969).
51. F.-l. Xu, J.-z. Duan, C.-g. Lin, and B.-r. Hou, *Journal of Iron and Steel Research, International,* **22** (8), 715-720 (2015).

334 **Table 1:** Composition of UNSS30400 and UNS32750 steel coupons.

335

Sample	Chemical Composition, %										
	Cr	**Ni**	**Mo**	**C**	**N**	**Mn**	**Si**	**Cu**	**P**	**S**	**Fe**
UNSS32750	24.0-26.0	6.0-8.0	3.0-5.0	0.03	.24-.32	1.2	0.8	0.5	0.035	0.02	Balance
UNSS30400	18.13	8.02	nil	0.02	0.077	1.35	0.35	nil	0.029	0.005	Balance

336

337

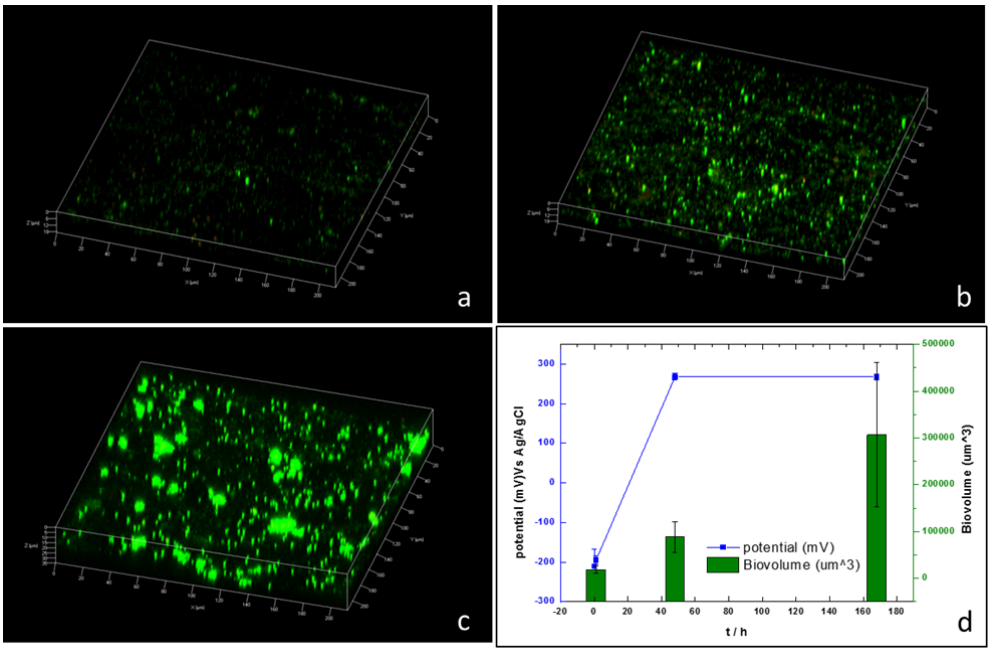

Figure 1: CLSM images of UNSS32750 in natural seawater at a) 1 h; b) 2 days and c) 7 days. d) bio-volume and open circuit potential after deployment.

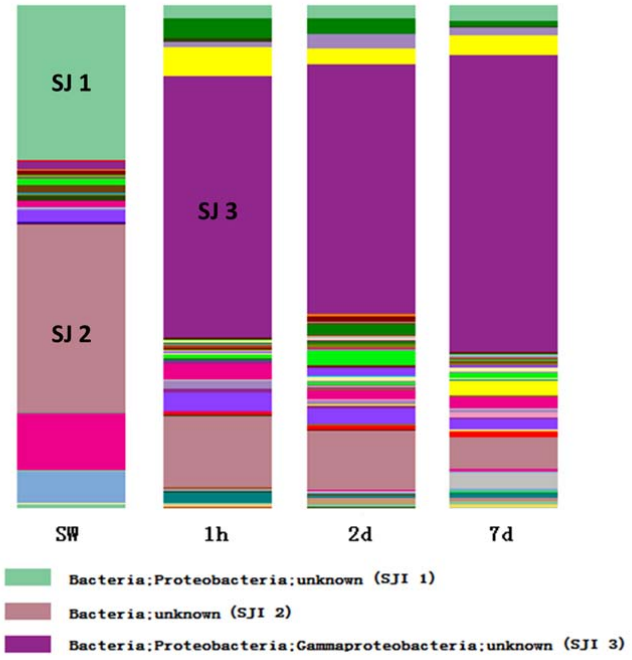

Figure 2: Bacterial composition of biofilms formed on UNSS32750 coupons. Each colour represents an individual OTU at the 97% identity threshold. The height of each section represents the relative abundance of the OTU in the samples.

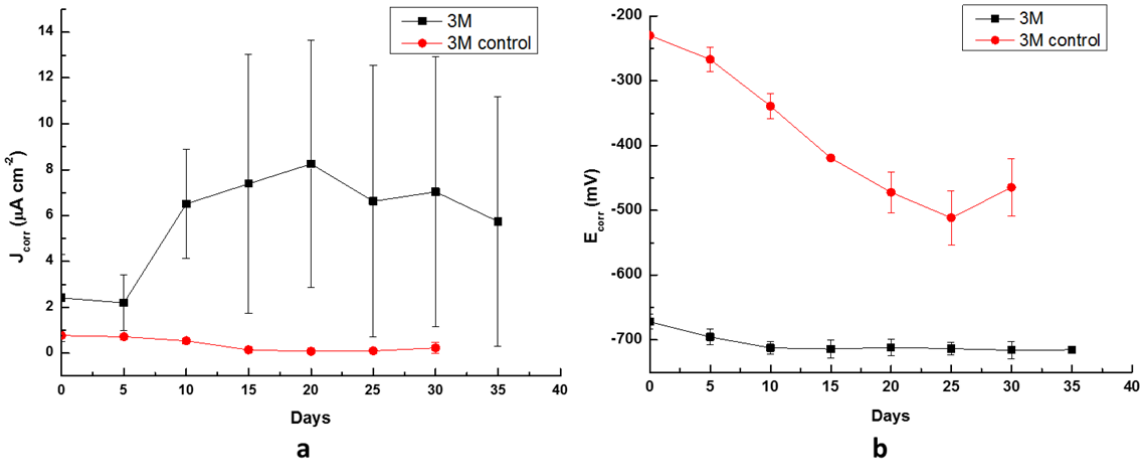

348

349 **Figure 3:** j_{corr} (a) and E_{corr} (b) of UNSS30400 across 35 days in 3M. Black trace corresponds to biotic

350 conditions and red trace corresponds to abiotic (sterile)

351

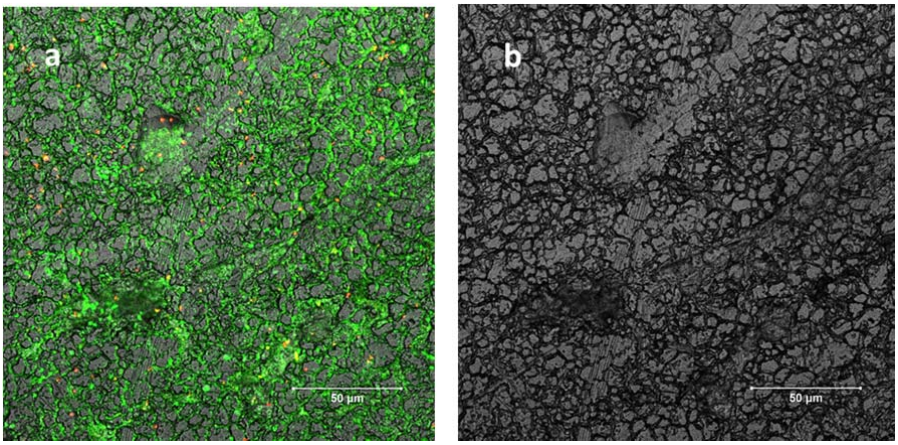

Figure 4: CLSM images of surface of UNSS30400 coupon after 35 days. Biofilm and surface (a); surface only (b) (400 × magnification).

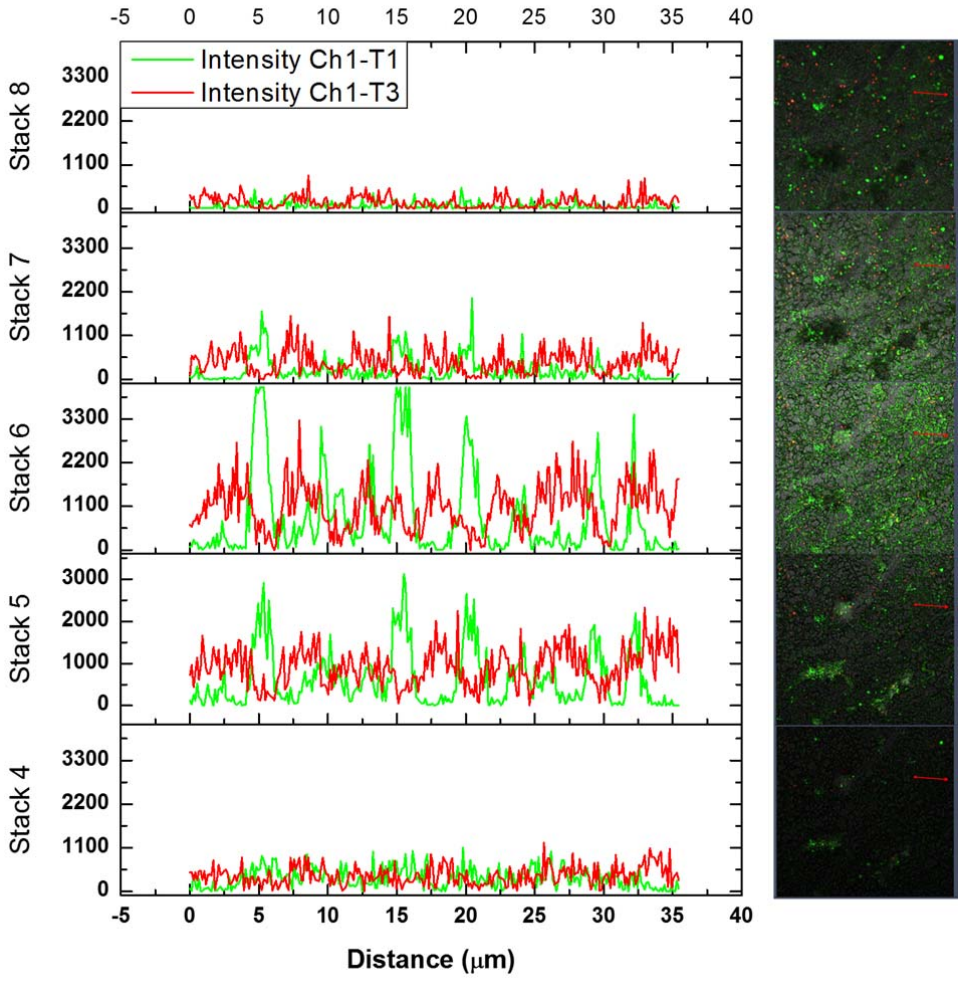

Figure 5: A typical intensity profile for reflection of the coupon (red trace) and the biofilm (green trace). The intensity profiles are measured across the red line (35 μm). Only the central stacks of the three-dimensional confocal images are reported [stack 4 to stack 8]. High values of red traces correspond to positive topographical features on the SS surface. High values of green trace correspond to high concentration of microbial cells. Biofilms is preferentially localized in negative topographical features on the SS surface.

365 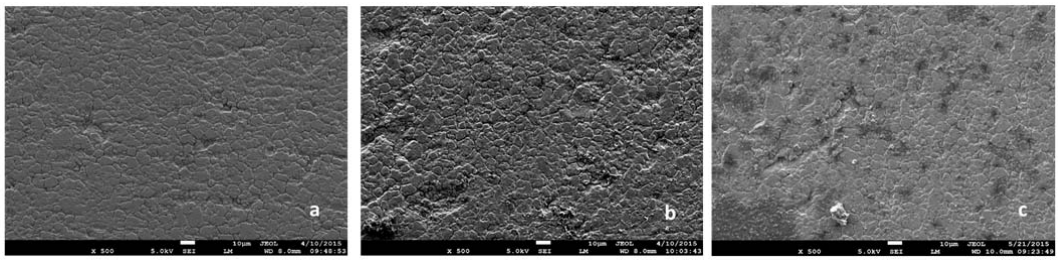

366 **Figure 6:** FESEM images for unpolished UNSS30400 coupons after 35 days (a). Control coupon on
367 day 0, (b). coupon on day 35 after cleaning off the biofilm, (c). Control coupon in sterile medium on
368 day 35.

369

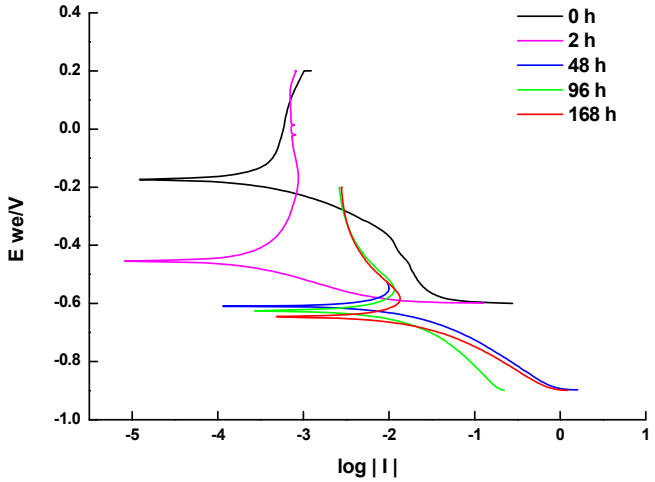

Figure 7: Tafel plots of representative UNSS30400 coupon in 3M at 40 rpm shaking across 7 days.

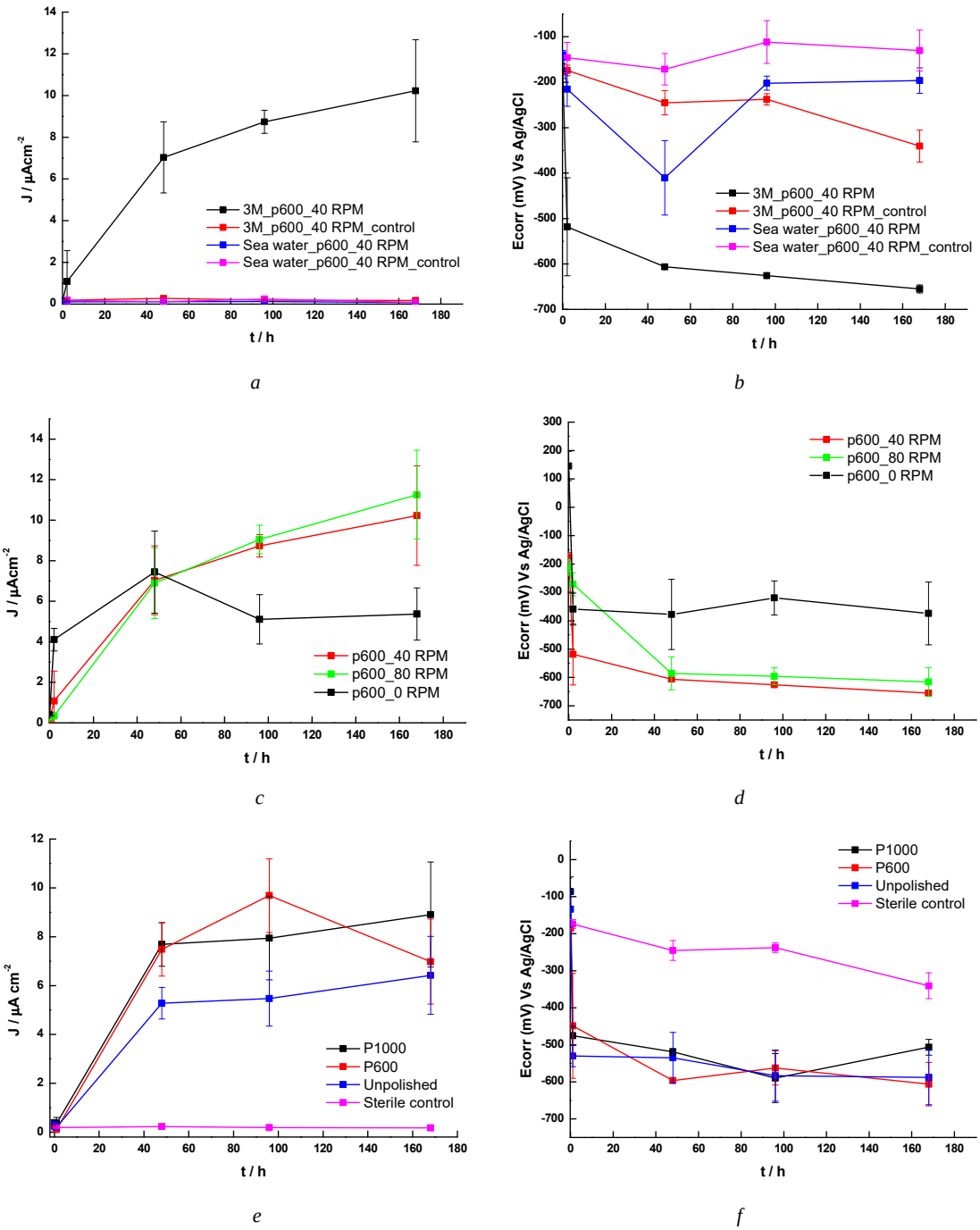

Figure 8: Effect of nutrient concentration on E_{corr} and j_{corr} for UNSS30400coupons (P600, 40 rpm, 3M vs. seawater, biotic Vs. sterile control) (a,b); effect of shaking speed (P600, effect of 0, 40 , 80 rpm) (c,d); effect of surface polishing (unpolished, P600, P1000, pre-soaked for 4 days) (e,f).